

## Probabilistic Seismic Hazard Assessment of City Center of Kayseri

Huseyin Cilsalar\*<sup>1</sup>, Ugur Temiz<sup>2</sup>,

\*<sup>1</sup> Yozgat Bozok University, Faculty of Engineering and Architecture, Department of Civil Engineering,  
YOZGAT

<sup>2</sup> Yozgat Bozok University, Faculty of Engineering and Architecture, Department of Geological Engineering,  
YOZGAT

(Alınış / Received: 27.10.2019, Kabul / Accepted: 13.06.2020, Online Yayınlanma / Published Online: 17.08.2020)

### Keywords

Probabilistic seismic hazard,  
Seismic hazard curve,  
Seismic hazard  
deaggregation,  
Kayseri

**Abstract:** Seismic hazard in city center of Kayseri is evaluated with probabilistic approach in this study. Earthquakes happened between 1900 and 2018 around the city are considered for the evaluation, and magnitude-recurrence relation of these events is obtained. Using a ground motion prediction equation, peak ground acceleration, spectral accelerations at period of 0.2 and 1 sec with different return periods are calculated and corresponding seismic hazard curves are demonstrated. Uniform hazard spectra are constructed and compared with those spectra obtained from Turkish seismic design code. Also, seismic hazard is deaggregated to distinguish how different magnitude and distances contribute expected hazard in the city center. Seismic hazard curves obtained in this study can be used to construct earthquake spectra for different return period earthquake events, and for the selection of ground motions to be used in dynamic analysis of structures. Results of seismic hazard deaggregation show that mean magnitudes contributing the hazard at the site considered are around 6.3 for peak ground acceleration and spectral acceleration at 0.2 sec, and 6.7 for the spectral acceleration at 1 sec period for both probability of exceedance of 2% and 10% in 50 years and soil types that have shear wave velocity of 760 m/s or higher.

## Kayseri İli Şehir Merkezinin Olasılıksal Sismik Tehlike Değerlendirmesi

### Anahtar Kelimeler

Olasılıksal sismik tehlike,  
Sismik tehlike eğrileri,  
Sismik tehlike  
ayrıştırılması,  
Kayseri

**Öz:** Bu çalışmada Kayseri ili şehir merkezindeki sismik tehlike olasılıksal yaklaşım ile değerlendirilmiştir. 1900 ve 2018 arası şehir çevresinde meydana gelen depremler değerlendirme için dikkate alınmış ve bu depremlerin magnitüd-frekans ilişkisi elde edilmiştir. Yer hareketi tahmin denklemi kullanarak farklı tekerrür periyotlarına sahip maksimum yer ivmesi, 0.2 ve 1 saniyeye karşılık gelen spektral ivmeler hesaplanmış ve bunlara ait sismik tehlike eğrileri gösterilmiştir. Üniform tehlike spektrumları elde edilmiş ve Türkiye deprem yönetmeliğinden elde edilen spektrumlarla karşılaştırılmıştır. Ayrıca, sismik tehlike, farklı magnitüd ve mesafelerin beklenen tehlikeye nasıl katkı yaptığını belirlemek için ayrıştırılmıştır. Bu çalışmada elde edilen sismik tehlike eğrileri, farklı tekerrür periyotlu depremler için spektrumların oluşturulmasında ve yapıların dinamik analizinde kullanılacak yer hareketlerinin seçiminde kullanılabilir. Sismik tehlike ayrıştırmasının sonuçları göstermektedir ki belirlenen alan için tehlikeye katkıda bulunan ortalama magnitüd değeri, ortalama kayma hızı 760 m/s ya da daha fazla olan zeminlerde, 50 yılda aşılma olasılığı %2 ve %10 olan maksimum yer ivmesi ve 0.2 saniye periyotlu spektral ivme için 6.3 civarında, 1 saniye periyotlu spektral ivme için 6.7 civarındadır.

\*İlgili Yazar, email: huseyin.cilsalar@bozok.edu.tr

## 1. Introduction

Structural analysis is critical to evaluate collapse performance, which requires having a model that can capture all failure modes and deterioration mechanisms properly, especially near collapse of the building. In addition, estimation of loads is also significant to the structural design. One of the most complicated load types that may act on a structure during the service life is earthquake load. Because it is dynamic and there is no clue beforehand where and when it may occur. These properties of earthquakes, along with many others, determine ground motions to be used in collapse or fragility analysis and this significant issue needs to be addressed before any structural analysis is performed. Also, earthquake spectra which form base for these analyses are mainly related with the expected earthquake.

However, there is no any information available at the time of design of a structure about future earthquakes. So, best estimation should be made based on the past events so that structures withstand against ground shaking. This estimation of future earthquakes are carried out using two different methods; deterministic and probabilistic seismic hazard analysis (PSHA). Former method is about to determine the worst-case earthquake scenario. This may seem simple at first. However, making a decision on just one event that has highest intensity on site is not an easy task. High magnitude events further away from the site can be more intense than nearby events with low magnitude. Hence, all different possible scenarios, occurring at different magnitude and locations, should be taken into account and decision should be made out of all these events.

Probabilistic seismic hazard analysis, on the other hand, is a tool that was developed to evaluate seismic hazard at a site considering magnitude and location uncertainties of future earthquakes based on probabilistic method, using earthquakes in the past. It was first introduced by C. Allin Cornell in 1968 [1], and instead of just one event, all earthquakes that may occur around the site are considered for the calculation, with different magnitude and locations. Its history, early and recent developments are summarized in [2]. In addition to earthquake magnitude and location, using a ground motion prediction relation, ground motion intensity and related statistics are computed such as probability of exceedance of acceleration at different structural periods. Combining all these results, seismic hazard for the considered site is calculated.

In this study, probabilistic seismic hazard analysis approach is used to evaluate seismic hazard of city center of Kayseri. Some similar studies are available in literature for different parts of Turkey [3-8]. Magnitude-recurrence relation is calculated using past events around city center, which happened between 1900 and 2018. These earthquakes are obtained from Disaster and Emergency Management Presidency (AFAD) [9]. All earthquakes occurred within radius of 150 km around the site are considered for calculation. Annual rate of exceedance of different ground motion intensities are also calculated and seismic hazard curves are illustrated for 43, 72, 475, and 2475-year return periods. Uniform hazard spectrum (UHS) is constructed using these seismic hazard curves and compared with those obtained from Turkish seismic design code (TSDC) [10] for different types of soils. Seismic hazard deaggregation procedure [11] is employed to have an idea of how different magnitudes and distance parameters are contributing hazard at city center and mean values of magnitudes and distances, contributing to hazard, are obtained.

## 2. Material and Method

Probabilistic seismic hazard analysis is performed considering five steps following;

- 1- First step is to identify each possible earthquakes source or sources that can produce earthquake which has possible damage to structure at site. These source or sources might be point, line and area, or combination of these three, in plane. However, more complex source models can also be assumed such as three dimensional sources which are computationally expensive.
- 2- All earthquakes happened in a time frame on the source, determined at first step, are obtained, and occurrence of each event, greater than a specific magnitude, per year is computed.
- 3- Depending on the source type, probability of location of an earthquake is calculated in this step.
- 4- Probability distribution of ground motion intensity such as peak ground acceleration (PGA), peak ground velocity (PGV) or spectral acceleration at a structural period of  $T$ ,  $S_a(T)$ , should be determined at this step. A ground motion prediction equation (GMPE) is needed for this calculation and it should be applicable to the site considered.
- 5- Last step is to combine all statistics obtained through Steps 1-4, and to compute mean annual rate of exceedance or seismic hazard curve of a ground motion intensity parameter considered at Step 4.

## 2.1 Seismic sources around the city and identification of the source

Kayseri and its vicinity in the Central Anatolia Region are under the influence of important fault zones. One of the most important fault zones is the NE-SW trending Central Anatolian Fault Zone with a left lateral strike slip within the continent that controls Kayseri and its vicinity and the eastern part of Central Anatolia (CAFZ) [12], as shown in Figure 1a. NE trending fault, which is approximately 730 km long and 2 to 80 km wide, consists of 24 segments while covering the Anatolian plate [13]. This fault zone is bending in the region of Kayseri and forms Erciyes pull-apart basin and Erciyes volcanic complex [13]. The Erciyes pull-apart basin is defined as an S-shaped active-growing depression area of approximately 35 km wide, 120 km long and 1.2 km deep [13], as illustrated in Figure 1b. It is controlled by important fault segments that control the western and eastern borders of this depression area in which Kayseri is located. The Kizilirmak-Erkilet and Yesilhisar fault segments of the OAFZ are bounded by the western part of the Erciyes pull-apart basin. Kizilirmak-Erkilet segment is 2-10 km wide, 170 km long and has a N50°E extension. The Yesilhisar fault segment is a normal strike component with an N-S extension and step morphology with a width of 8 km, length of 60 km from several hundred meters. The eastern part of the basin is bordered by Dunderli-Erciyes and Develi subfault segments, which are found under the Dometmetas fault segment and lower branches. Dunderli-Erciyes fault segment is a left lateral strike fault with normal strike component is 83 km long and N17°E trend. The Develi fault segment is an oblique-slip with normal fault, its extension is NNE and has a length of approximately 104 km [13] Figure 1b.

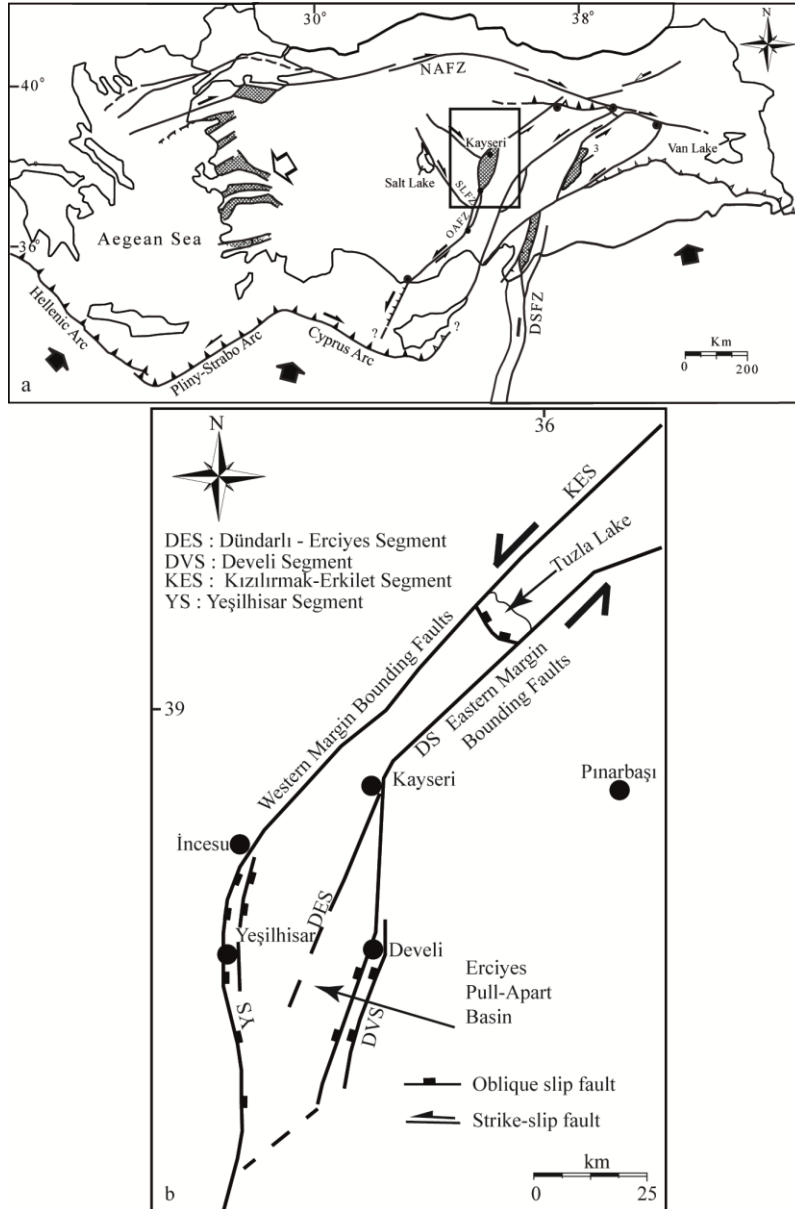


**Figure 1.** a) Simplified neotectonics map of Turkey and the environment (DSFZ: Dead Sea Fault Zone, SLFZ: Salt Lake Fault Zone, NAFZ: North Anatolian Fault Zone (modified from [12]), b) Neotectonic map of the Erciyes pull-apart basin included in the Central Anatolian Fault Zone modified from [13]).

Although the exact location and magnitude of the outer center is not known in Kayseri and its vicinity, 10 historical earthquakes were recorded, and these are given in Table 1 [14]. These earthquakes occurred in the vicinity of Niğde, Develi, Kayseri, and Sivas.

**Table 1.** Historical earthquakes in Central Anatolia between the years 240-1900 [14]

Date (year/month/day)	Coordinates	Location	Intensity
240		Kayseri-Sivas	IX
1104		Niğde	IX
1205	38.70-35.50	Kayseri	VIII
1695.01.01		Sivas	
1704.06.09		Kayseri	
1714		Kayseri	VII
1717.05.09	38.70-35.50	Kayseri	VIII
1754.09.16	39.75-37.00	Kangal (Sivas)	VII
1779.03.14		Divriği (Sivas)	
1835.08.23	38.30-35.50	Develi (Kayseri)	VIII

A catalogue is formed using the data obtained from [9], for the seismic hazard evaluation of city center. This catalogue includes events between 1900 and 2018, and magnitude of these earthquakes are higher than 4. It is observed that all earthquakes are scattered all around the city center, and there is not an accumulation of events on a fault segment dominantly. So, it is reasonable to assume an area source model for the earthquakes. Hence, line source is omitted. A circle with a radius of 150 km is defined as area source. Occurrence of each magnitude of earthquakes in the area per year is key parameter for the PSHA calculation.

Earthquake catalogue includes different types of magnitude definition and they are needed to be converted a single type that can be used in ground motion prediction equation. So, all magnitudes are converted to the moment magnitude,  $M_w$ . Conversion relations proposed by [15] are used in this study as given in Equation 1.

$$\begin{aligned}
 M_w &= 2.25M_b - 6.14 \\
 M_w &= 1.27M_d - 1.12 \\
 M_w &= 1.57M_l - 2.66 \\
 M_w &= 0.54M_s + 2.81
 \end{aligned} \tag{1}$$

After conversion of magnitudes, they range approximately from 3 to 6.5 within the area source that is previously defined. All these data are ranked to obtain annual occurrence of events within the time frame considered in the catalogue. Recurrence relation is calculated by Gutenberg-Richter recurrence law [16], as given in Equation 2.

$$\log_{10}(\lambda_m) = a - bM \tag{2}$$

In this equation  $M$  is the magnitude of an earthquake,  $a$  and  $b$  are regression coefficients and  $\lambda_m$  is the rate of earthquakes with magnitude  $M$ . Cumulative distribution function of a magnitude can be estimated based on  $a$  and  $b$  coefficients in Equation 2. However, it is unrealistic to assume that a source can produce any magnitude. Therefore, event magnitudes are needed to be limited so that reasonable estimation can be made with the data. In this study, only magnitudes between 4 and 7 are considered. Earthquakes which have magnitudes less than 4 are not expected to damage a structure. So, magnitudes below this omitted for the sake of computational convenience. On the other hand, upper value is limited to be 7 due to lack of data at high magnitudes. Considering this bounding, cumulative distribution function of can be expressed depending on the coefficients in Equation 2.

$$F_m = \frac{1 - 10^{-b(m-m_{min})}}{1 - 10^{-b(m_{max}-m_{min})}} \quad m_{min} < m < m_{max} \quad (3)$$

$F_m$  is cumulative distribution function of magnitude,  $m$ ,  $m_{max}$  and  $m_{min}$  are the maximum and minimum magnitudes that source can produce, respectively. Figure 2 shows annual rate of exceedance of earthquakes magnitudes as result of the computation.

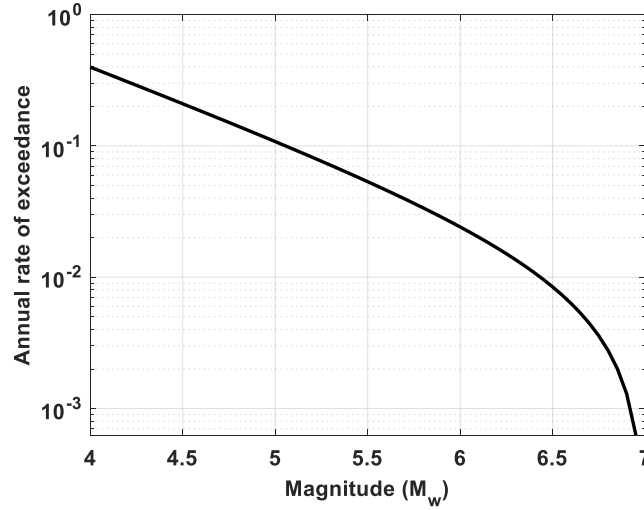


Figure 2. Magnitude recurrence relation based on bounded Gutenberg-Richter law

## 2.2. Ground Motion Prediction Equation

After distribution of earthquake magnitudes and locations are determined, next step is to evaluate statistics of specific ground motion intensities. This requires a ground motion prediction equation (GMPE) which can be used for the site under consideration for seismic hazard. GMPE is a formulation to calculate different intensities of ground motion depending on some parameters such as, magnitude, distance, fault type, soil type etc.

There are some ground motion prediction equations available, proposed for Turkey, [17-20] in horizontal direction. A prediction relation for vertical ground motions in Turkey is proposed by Kalkan and Gülkan [21], and other studies are also investigated vertical ground motion in Turkey [22-23]. In this study, proposed method by Kale et al. [20] in horizontal direction is used. General form of this prediction relation is given in Equation 4. This model have controlling parameters of magnitude scaling, ( $f_{mag}$ ), geometric decay, ( $f_{dis}$ ), type of fault mechanism on site ( $f_{sof}$ ), site effects ( $f_{site}$ ) and elastic attenuation ( $f_{att}$ ) to calculate logarithmic mean value of a ground motion intensity. Here,  $Y$  can be any of peak ground acceleration (PGA, g), peak ground velocity (PGV, cm/s) or spectral accelerations at different structural period. This model can predict ground motion parameter of an earthquake that have moment magnitude ( $M_w$ ) between 4 to 8 and Joyner-Boore ( $R_{JB}$ ) distance up to 200 km. So, in this study all distances are calculated as Joyner-Boore distance to be consistent with the prediction relation used. Soil type is also another input parameter for this prediction relation and shear wave velocity at upper 30 m part, ( $V_s$ )<sub>30</sub>, of the soil is considered for calculation. Change in PGA value with respect to distance and magnitude is illustrated in Figure 3 for ( $V_s$ )<sub>30</sub> value of 760 m/s.

$$\ln Y = f_{mag} + f_{dis} + f_{sof} + f_{aat} + f_{site} \quad (4)$$

There are six different types of soils defined in TSDC, from ZA to ZF, and classification depends on ( $V_s$ )<sub>30</sub> and other soil properties. In this study, values for ( $V_s$ )<sub>30</sub> are selected to be 1500 m/s, 760 m/s, 360 m/s and 180 m/s. These values represent transition between soil types of ZA-ZB, ZB-ZC, ZC-ZD and ZD-ZE, respectively. Seismic hazard curves and uniform hazard spectra for each types of soil are constructed and compared with the TSDC.

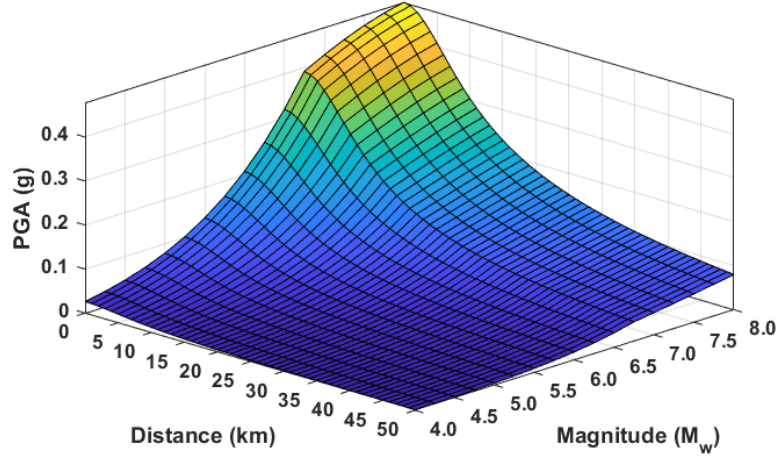


**Figure 3.** PGA change depending on magnitude and distance for used ground motion prediction equation

Standard deviation of ground motion intensity is also calculated with this proposed GMPE by [20], which is also used to determine probability of exceedance of ground motion parameters for the PSHA calculation.

## 2.2. Seismic hazard curves

Last part of probabilistic seismic hazard analysis is to combine all information obtained in the previous steps. Probability density functions of magnitude,  $f_m(m)$ , distance,  $f_r(r)$  and a ground motion parameter for a distinct value of  $m$  and  $r$ ,  $P(IM > x|m, r)$ , which is calculated from a GMPE, are combined all together to obtain probability of an intensity measure, IM, being greater than an arbitrary value of  $X$ , as shown in Equation 5.

$$P(IM > X) = \int_{m_{min}}^{m_{max}} \int_0^{r_{max}} P(IM > x|m, r) f_m(m) f_r(r) dr dm \quad (5)$$

However, this equation does not include any information about frequency of an event or annual rate of exceedance. Including magnitude-recurrence relation of the source in the equation, Equation 5 can be written as;

$$\lambda(IM > X) = \lambda(M > m_{min}) \int_{m_{min}}^{m_{max}} \int_0^{r_{max}} P(IM > x|m, r) f_m(m) f_r(r) dr dm \quad (6)$$

In this equation  $\lambda(M > m_{min})$  is the rate of occurrence of earthquakes in a source with magnitudes greater than  $m_{min}$  and it is calculated as given in Equation 7.

$$\lambda(M > m_{min}) = 10^{a-bm_{min}} \quad (7)$$

$(IM > X)$  gives rate of an intensity measure greater than  $X$ . Considering all sources and discrete distribution of magnitude and distance Equation 6 is written for the discretized values of magnitude and distance as given in Equation 8.

$$\lambda(IM > X) = \sum_{i=1}^{N_{sources}} \lambda(M_i > m_{min}) \sum_{j=1}^{N_M} \sum_{k=1}^{N_R} P(IM > x|m_j, r_k) P(M_i = m_j) P(R_i = r_k) \quad (8)$$

$N_{sources}$  is number sources considered,  $N_M$  and  $N_R$  denote number of magnitudes and distances discretized at  $M_j$  and  $R_k$ . Summation of these quantities in Equation 8 yields mean annual rate of exceedance of a ground motion intensity,  $\lambda(IM > X)$ . Repetitive calculation of this step gives seismic hazard curve for considered IM. Detailed explanation for introduction to PSHA and related calculations, and extension of the method to deaggregate seismic hazard can be found in [24].

### 3. Results

Seismic hazard curves for four different soil types are computed. Moreover, uniform hazard spectrum (UHS) for these soil types is given. In TSDC, four different earthquake levels are defined from DD-1 to DD-4. DD-1 is the highest earthquake level, defined in the code, with 2% probability of exceedance in 50 years. Other levels DD-2, DD-3 and DD-4 have 10%, 50% and 68% of probability of exceedance with return periods of 475, 72 and 43 years, respectively. So, these time values are used for return period of the earthquakes to compute UHS.

Figure 4 shows seismic hazard curves for four different types of soil and three different ground motion intensities. Horizontal lines are added in the figures to show time horizons determined to construct UHS.

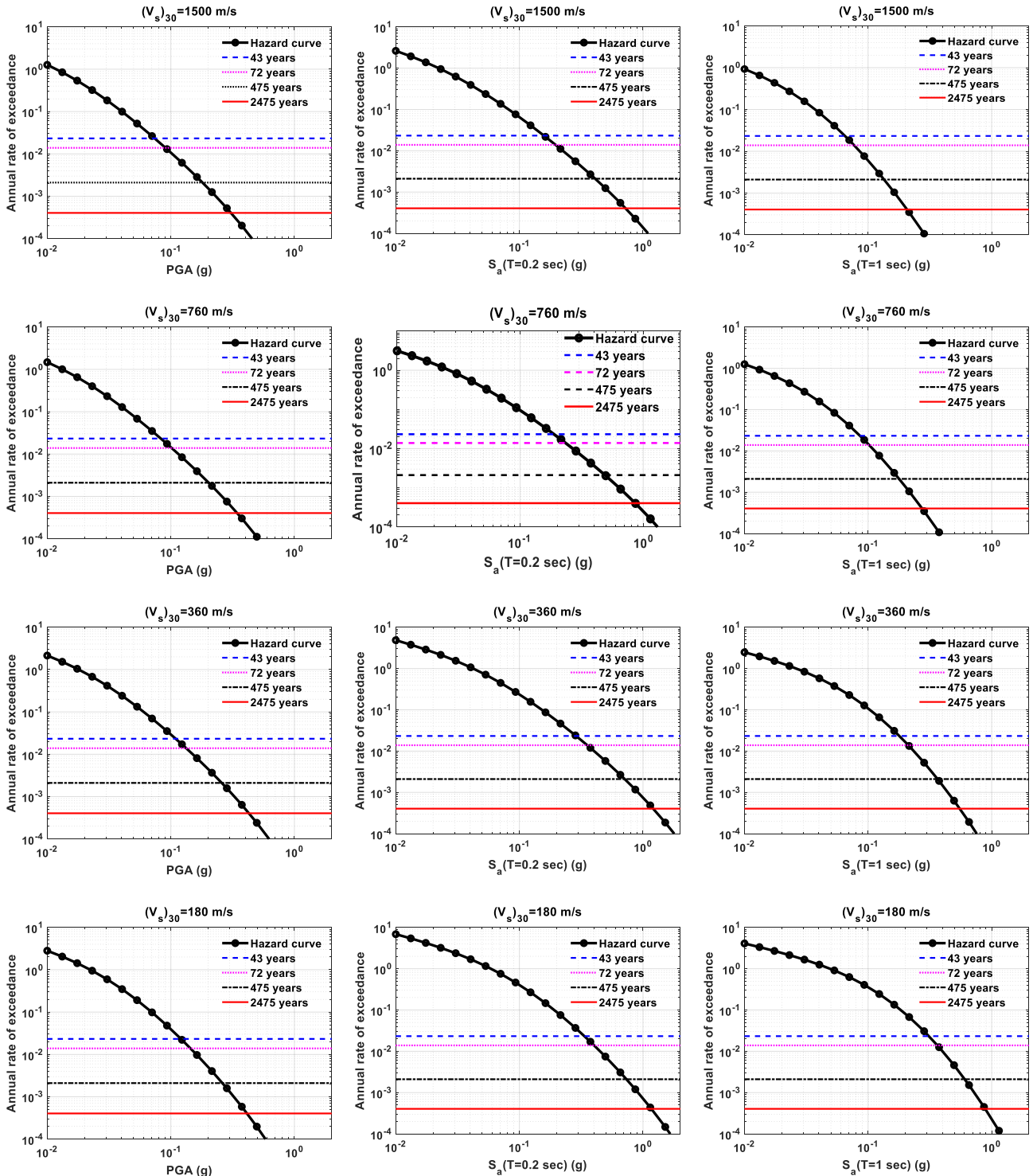


Figure 4. Seismic hazard curves for different ground motion intensities and soil types

Design spectra are based on short and long period spectral acceleration coefficients, which are given as spectral accelerations at 0.2 and 1 sec as per TSDC. So, seismic hazard curves are calculated for  $S_a(T = 0.2 \text{ sec})$ , and  $S_a(T = 1 \text{ sec})$ , in addition to PGA. Seismic hazard curves for these three different ground motions with different soil parameters in hand, spectra for any return period event can be constructed without any sophisticated calculations.

Uniform hazard spectrum (UHS) is obtained based on a target return period or rate of exceedance. Accelerations values on different seismic hazard curves corresponding to distinct return period are selected and plotted against structural period. So, each point on a UHS has the same annual rate of exceedance. Following Figures 5-8 show uniform hazard spectra, each one of these correspond to different earthquake levels defined in TSDC, and soil types. Observed uniform hazard spectra are also compared by the design spectra from TSDC. In these figures  $P_{ex}$  is the probability of exceedance of each point on the spectrum.

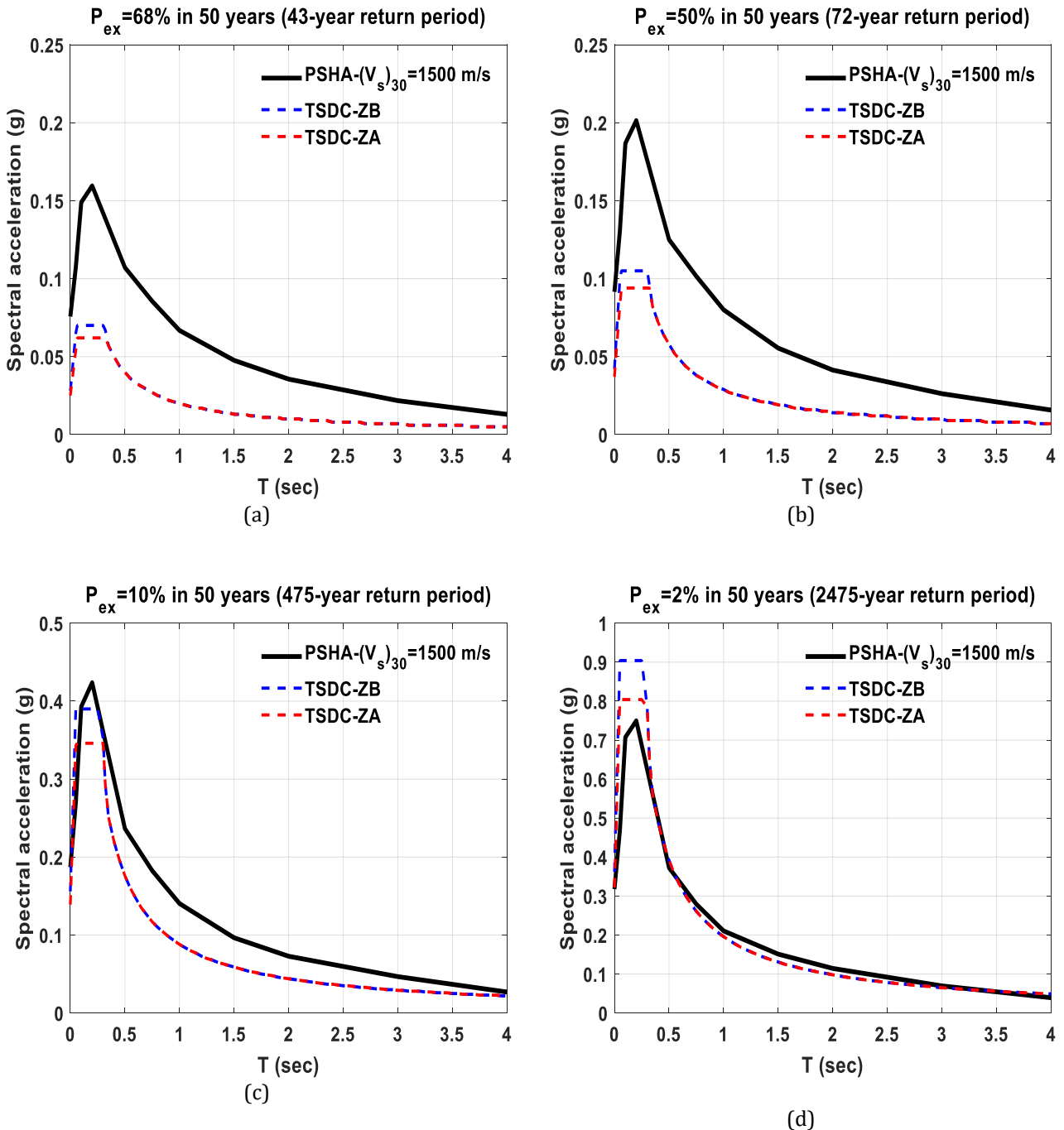
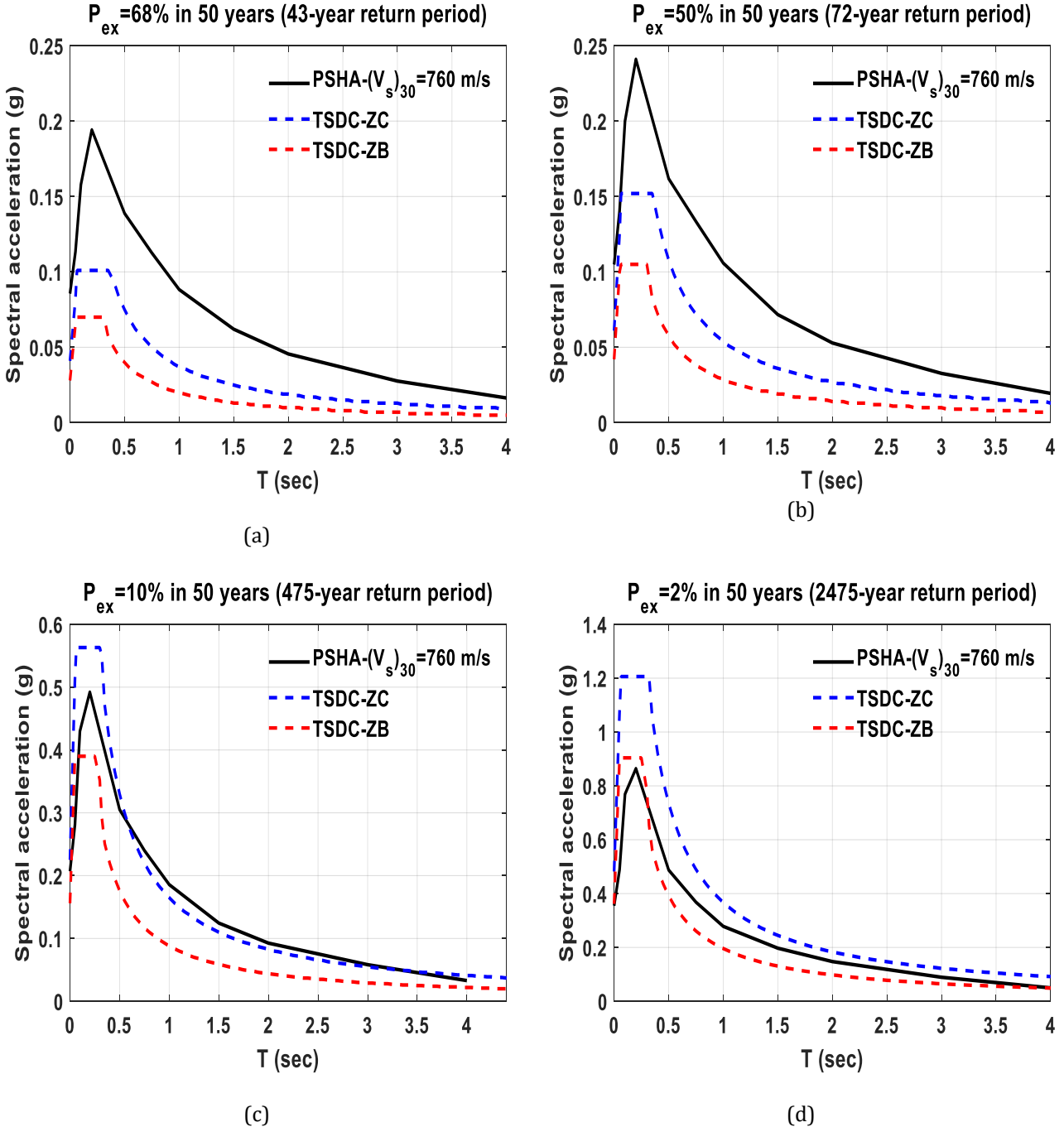


Figure 5. Comparison of UHS and design spectra for different return period event,  $(V_s)_{30} = 1500 \text{ m/s}$   
 (a) 43-year event (b) 72-year event (c) 475-year event (d) 2475-year event

It is observed that PSHA predicts higher values of accelerations for 43 and 72-year return period event for almost all structural periods and soil types, although, it is converging to the design spectra at periods around 4 sec. Constant acceleration range for the spectra obtained by PSHA is observed to be wider for these earthquake levels, as well. For earthquakes level of DD-1 and DD-2, PSHA results fall between two spectra at low periods, and almost same with them in large periods. Here please note that shear wave velocity shown in the graphs are the transition value between two soil types given in the same figure, and these soil types are defined in TSDC.



**Figure 6.** Comparison of UHS and design spectra for different return period event,  $(V_s)_{30} = 760$  m/s  
 (a) 43-year event (b) 72-year event (c) 475-year event (d) 2475-year event

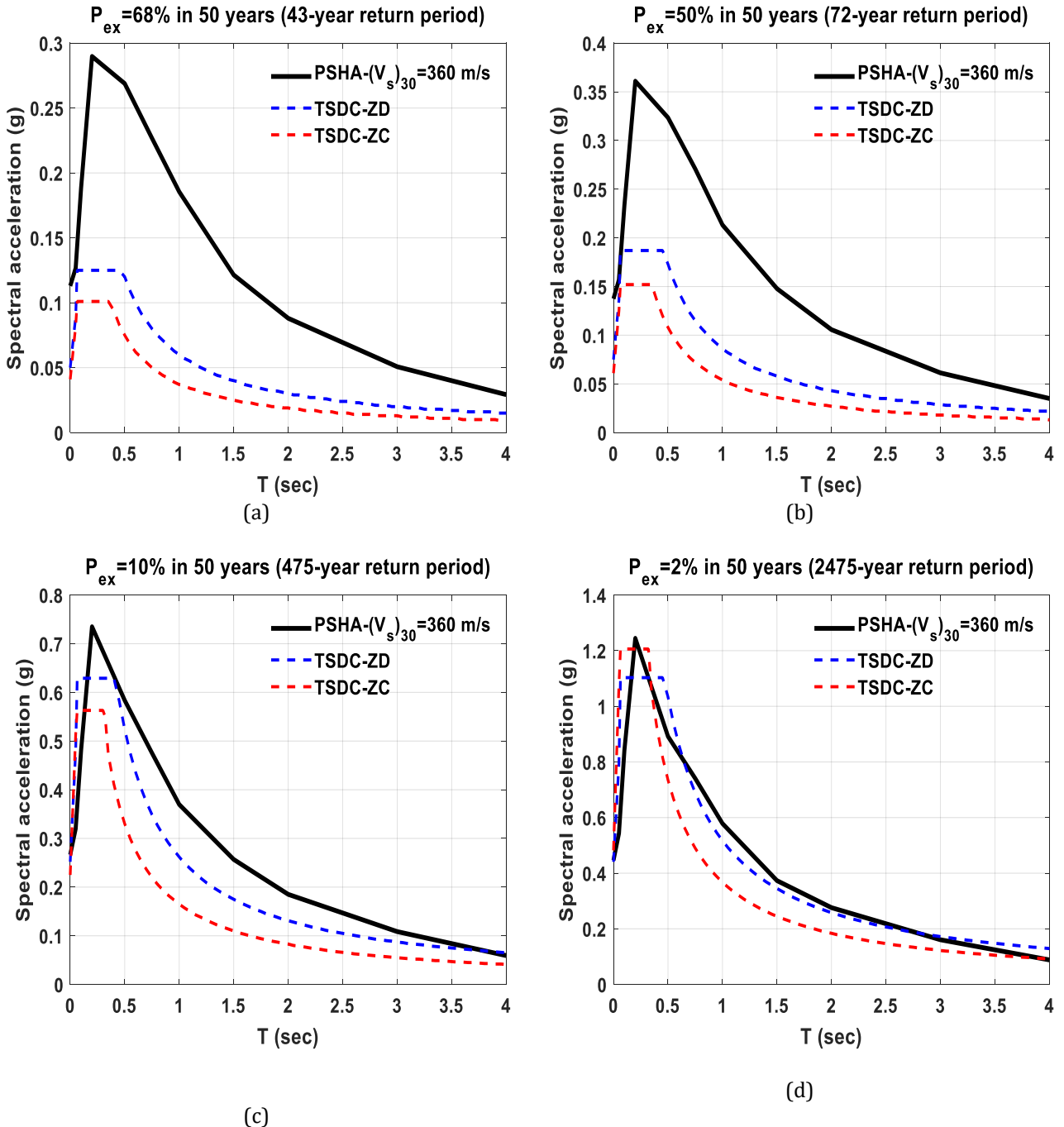
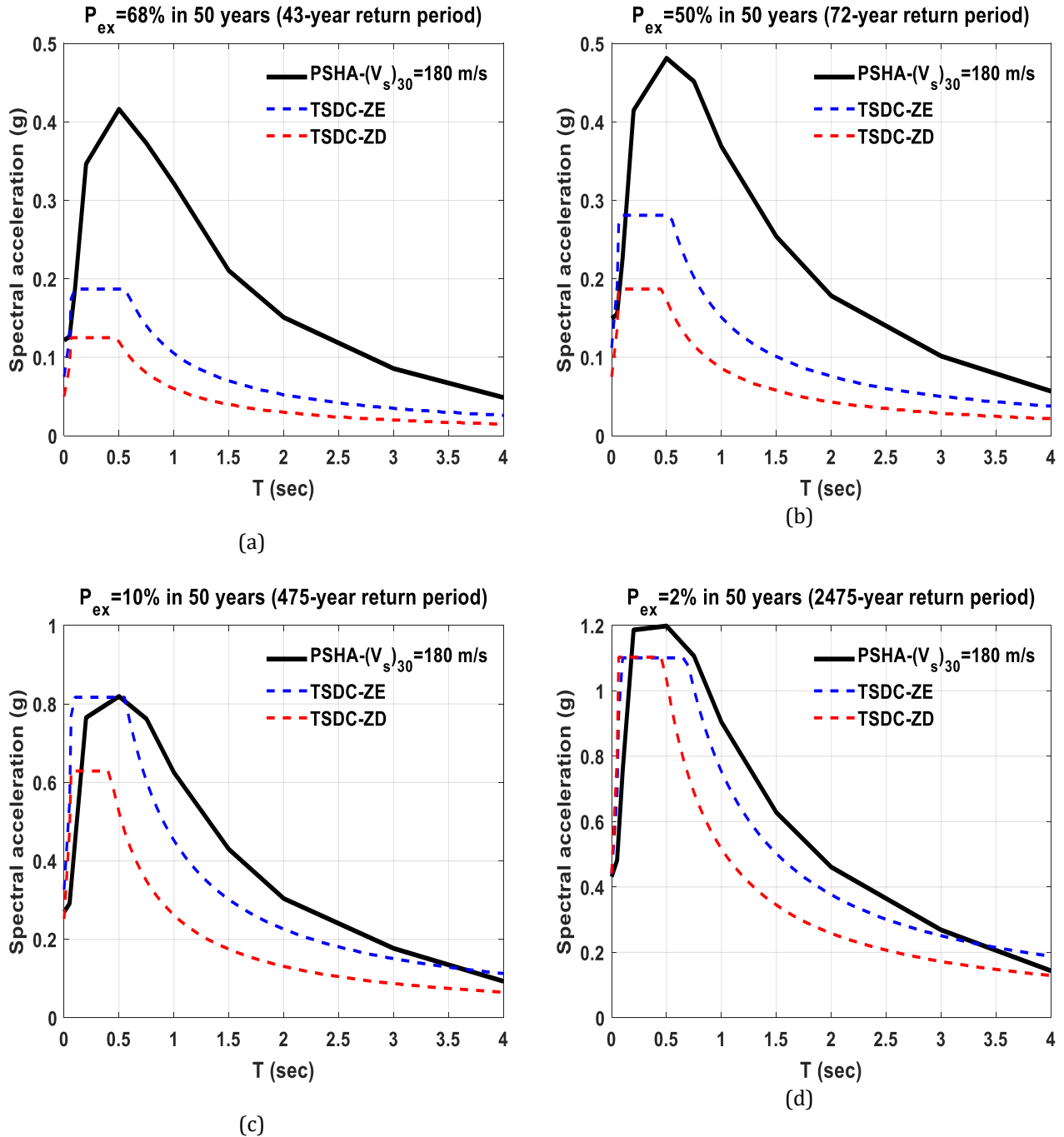


Figure 7. Comparison of UHS and design spectra for different return period event, ( $V_s$ )<sub>30</sub> = 360 m/s  
 (a) 43-year event (b) 72-year event (c) 475-year event (d) 2475-year event



**Figure 8.** Comparison of UHS and design spectra for different return period event, ( $V_s$ )<sub>30</sub> = 180 m/s  
 (a) 43-year event (b) 72-year event (c) 475-year event (d) 2475-year event

Seismic hazard at the site is deaggregated for the events that have 2% and 10% probability of exceedance in 50 years for the soil types with shear wave velocity of 760 m/s and 150 m/s. Contribution of magnitude-distance pairs to the hazard is calculated, and mean values of these are given in Table 2 for peak ground acceleration, and spectral accelerations at structural period of 0.2 and 1 second. For PGA, mean magnitude values are about 6.3, for short and long period spectral accelerations, it is around 6.25 and 6.70, respectively. Mean values of distances for PGA and short period spectral acceleration are around 14 km in 2475-year event and it is higher for 475-year event as expected. Distance values contributing to hazard, spectral acceleration at 1 sec structural period, is observed to be around 41 km and 53 km for 2475 and 475-year events, respectively.

**Table 2.** Mean values of magnitude-distance contributing to hazard

Vs (m/s)	IM	Parameter	Probability of exceedance in 50 years	
			2%	10%
760	PGA	$M_w$	6.32	6.29
		$R (km)$	14.34	20.19
	$S_a(T = 0.2 \text{ sec})$	$M_w$	6.27	6.23
		$R (km)$	14.24	19.75
	$S_a(T = 1 \text{ sec})$	$M_w$	6.70	6.69
		$R (km)$	41.57	53.28
1500	PGA	$M_w$	6.32	6.28
		$R (km)$	14.30	20.44
	$S_a(T = 0.2 \text{ sec})$	$M_w$	6.28	6.24
		$R (km)$	13.95	19.45
	$S_a(T = 1 \text{ sec})$	$M_w$	6.70	6.69
		$R (km)$	41.56	53.10

#### 4. Discussion and Conclusion

Seismic hazard evaluation of city center of Kayseri is performed in the paper using probabilistic seismic hazard analysis approach. An earthquake catalogue is formed within a time frame and area source with radius of 150 km is defined for potential earthquakes around the city. Annual occurrence of each magnitude in the data and probability distribution of location of earthquakes are calculated.

Seismic hazard curves for PGA and spectral accelerations at period of 0.2 and 1 sec are illustrated for different soil types depending on shear wave velocities, which represent boundary between different soil types. Also, UHSs are constructed and compared with the design spectrum given in TSDC. Results of PSHA tend to yield higher values for low return period event for almost all structural periods, although it is relatively closer to code spectra for high periods. It is also observed that constant acceleration period region in UHS obtained from PSHA tend to be wider. In addition to seismic hazard curves and UHSs, seismic hazard at the site considered is deaggregated and mean values of magnitude-distance pairs contributing the hazard are calculated. Mean values of magnitude contributing the hazard at the site for two different soil types are around 6.3 for PGA and  $S_a(T = 0.2 \text{ sec})$ , and 6.7 for  $S_a(T = 1 \text{ sec})$ . These values of magnitudes are valid for events with 475 and 2475 years return period. In addition, another deaggregation parameter, R, is also calculated to evaluate how different distance values are contributing the hazard. Mean values of R parameter are around 14 km and 20 km for PGA values that have 2% and 10% of probability of exceedance in 50 years in those soil types which have 760 m/s or higher shear wave velocity.

Results of this paper can be used to compute seismic hazard of peak ground acceleration, spectral accelerations at 0.2 and 1 sec for different soil types and return periods. Uniform hazard spectrum can also be constructed for different level of earthquakes, and ground motions to be used for collapse evaluation can be selected accordingly.

#### References

- [1] Cornell, C. A. 1968. Engineering Seismic Risk Analysis. Bulletin of the Seismological Society of America, 58(5), 1583-1606.
- [2] McGuire, R. K. 2007. Probabilistic seismic hazard analysis: Early history. Earthquake Engineering & Structural Dynamics, 37(3), 329 - 338.
- [3] Kartal, R. F., Kilic, T., Kadiroglu, F.T. 2014. Olasılık ve İstatistik Yöntemler ile Mersin İlinin Sismik Tehlikesinin Tahmini. 1. Türkiye Deprem Mühendisliği ve Sismoloji Konferansı, 11-14 Ekim 2011 - ODTÜ - ANKARA.
- [4] Kartal, R. Ozyazicioglu, M., Kilic, T. 2015. Konaklı Kayak Merkezi (Erzurum) için Olasılıksal Sismik Tehlike Analizi. 3. Türkiye Deprem Mühendisliği ve Sismoloji Konferansı, 14-16 Ekim 2015 - DEÜ-İZMİR.

- [5] Kutanis, M., Ulutas, H., Isik, E. 2018. PSHA of Van province for performance assessment using spectrally matched strong ground motion records. *Journal of Earth System Science*, 127:99.
- [6] Erdik, M., Demircioğlu, K., Şeşetyan, K., Durukal, E., Siyahi, B. 2004 .Earthquake hazard in Marmara region, Turkey. *Soil Dynamics and Earthquake Engineering*, 1(24), 605-631.
- [7] Kalkan, E., Gülkan, P., Yılmaz, N., Çelebi, M. 2009. Reassessment of probabilistic seismic hazard in the Marmara Region. *Bulletin of Seismological Society of America*, (4)99, 2127-2146.
- [8] Harman, E. 2015. Sakarya ili için olasılığa dayalı sismik tehlike analizi. *SAÜ Fen Bilimleri Dergisi*, 20(1), 23-31.
- [9] Afet ve Acil Durum Yönetimi Başkanlığı Deprem Dairesi Başkanlığı (AFAD). AFAD deprem kataloğu, <https://deprem.afad.gov.tr/depremkatalogu>. (Last accessed: 23.11.2019)
- [10] Türkiye Bina Deprem Yönetmeliği 2019. Afet ve Acil Durum Yönetimi Başkanlığı (AFAD), [https://www.afad.gov.tr/kurumlar/afad.gov.tr/2309/files/TBDY\\_2018.pdf](https://www.afad.gov.tr/kurumlar/afad.gov.tr/2309/files/TBDY_2018.pdf). (Last accessed: 23.11.2019)
- [11] Bazzurro, P., Cornell, C. A. 1999. Disaggregation of Seismic Hazard, *Bulletin of Seismological Society of America*. (89)2, 501-520.
- [12] Koçyiğit, A, Beyhan, A., 1998. A new intracontinental transcurrent structure: the Central Anatolian Fault Zone, Turkey, *Tectonophysics*. 284(3-4),317-336.
- [13] Koçyiğit, A, Erol, O., 2001. A tectonic escape structure: Erciyes pull-apart basin, Kayseri, central Anatolia, Turkey. *Geodinamica Acta*, 14(1-3), 133-145.
- [14] Soysal, H., Sipahioğlu,S., Kolçak, D.,Altınok, Y.,1981. Türkiye ve çevresinin tarihsel deprem kataloğu (M.Ö. 2100 - M.S. 1900). TÜBİTAK yayınları, 563. Cilt, 86.
- [15] Deniz, A. & Yucemen, M.S. 2010. Magnitude conversion problem problem for Turkish earthquake data. *Natural Hazards*, 55(2), 33-352.
- [16] Gutenberg, B., Richter, C. F. 1944. Frequency of earthquakes in California. *Bulletin of the Seismological Society of America*, 34(4), 185-188.
- [17] Cagnan, Z., Akkar, S. A. 2010. Local Ground-Motion Predictive Model for Turkey, and Its Comparison with Other Regional and Global Ground-Motion Models, *Bulletin of Seismological Society of America*, 100(6), 2978-2995.
- [18] Gülerce, Z., Kargoiğlu, B., Abrahamson, N. A. 2016 Turkey-Adjusted NGA-W1 Horizontal Ground Motion Prediction Models. *Earthquake Spectra*, 32(1), 75-100.
- [19] Kalkan, E., Gülkan, P. 2004 Site-Dependent Spectra Derived from Ground Motion Records in Turkey. *Earthquake Spectra*, 20(4), 1111-1138.
- [20] Kale, Ö., Akkar, S., Ansari, A., Hamzehloo, H. 2015. A Ground-Motion Predictive Model for Iran and Turkey for Horizontal PGA, PGV, and 5% Damped Response Spectrum: Investigation of Possible Regional Effects, *Bulletin of the Seismological Society of America*. 105(2A), 963-980.
- [21] Kalkan, E., Gülkan, P. 2004 Empirical Attenuation Equations for Vertical Ground Motion in Turkey. *Earthquake Spectra*, 20(3), 853-882.
- [22] Alipour, N. A., Sandikkaya, M. A., Gülerce, Z. 2019. Ground Motion Characterization for Vertical Ground Motions in Turkey—Part 1: V/H Ratio Ground Motion Models. *Pure and Applied Geophysics*, 1-22. <https://doi.org/10.1007/s00024-019-02324-y>.
- [23] Gülerce, Z., Alipour, N. A., Sandikkaya, M. N. 2019. Ground Motion Characterization for Vertical Ground Motions in Turkey—Part 2: Vertical Ground Motion Models and the Final Logic Tree. *Pure and Applied Geophysics*, 1-19. <https://doi.org/10.1007/s00024-019-02353-7>.
- [24] Baker, J. W. 2015. Introduction to Probabilistic Seismic Hazard Analysis. White Paper Version 2.1, 77 pp.